Volume 23
Number 38
14 October 2025
Pages 8583-8810

Organic & Biomolecular Chemistry

rsc.li/obc

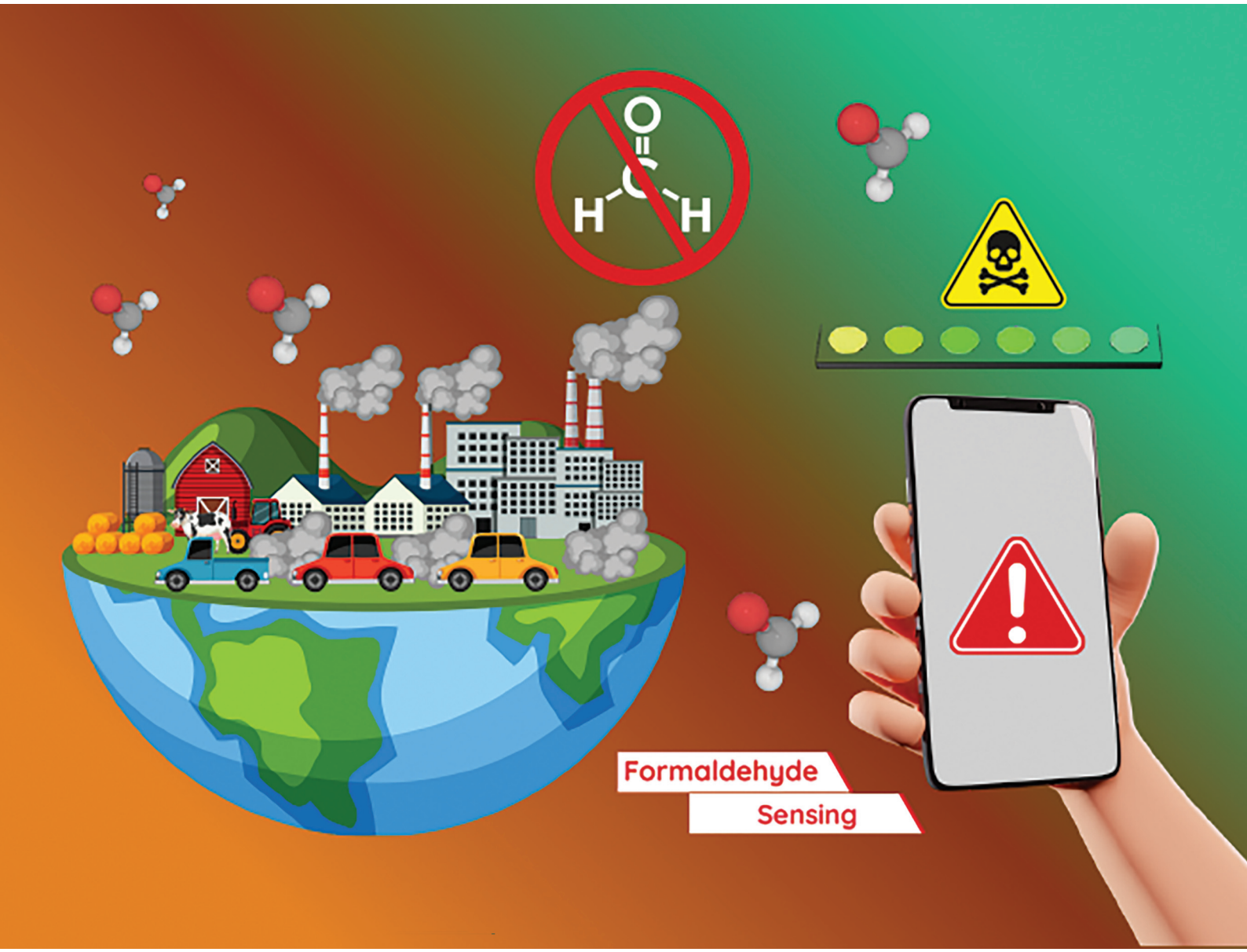

ISSN 1477-0520

ROYAL SOCIETY OF CHEMISTRY

REVIEW ARTICLE
Alessia Cavallaro, Giuseppe Trusso Sfrazzetto *et al.*
Formaldehyde sensing by fluorescent organic sensors

Organic & Biomolecular Chemistry

ROYAL SOCIETY OF CHEMISTRY

REVIEW

View Article Online
View Journal | View Issue

Cite this: *Org. Biomol. Chem.*, 2025, **23**, 8592

Formaldehyde sensing by fluorescent organic sensors

Rossella Santonocito, [a] Andrea Pappalardo, [a,b] Nunzio Tuccitto, [a] Alessia Cavallaro *[a] and Giuseppe Trusso Sfrazzetto *[a,b]

Formaldehyde is a simple molecule that can be found in different environments, having several toxic effects on both the environment and, unfortunately, humans. Therefore, the development of formaldehyde detection methods is fundamental. For this purpose, optical sensors are used, which are practical, fast and easy-to-use devices. The ideal sensor should exhibit high selectivity, sensitivity and short response time. This review summarizes the recent development in this field, highlighting the sensing properties of the systems in terms of sensitivity, selectivity and limit of detection. A comparison between the reported sensors in terms of efficiency of detection mechanisms and optical performance of different fluorophores is provided. Future perspectives of formaldehyde detection by optical probes are also provided, focusing on the current limitations that should be solved to obtain an ideal formaldehyde sensor.

Received 22nd May 2025,
Accepted 21st July 2025

DOI: 10.1039/d5ob00858a

rsc.li/obc

Introduction

From a structural point of view, formaldehyde (FA) is the simplest aldehydic compound that can be found in some biological pathways as well as in several foods due to its preservative properties. It was first described in 1855, while the first synthesis of methanol was performed in 1867 in Germany. FA is currently synthetized on a large scale by the oxidation of methane or methanol in the presence of a catalyst.[1] It is a gas at room temperature, but it shows good solubility in water, ethanol, and other polar organic solvents. FA is also produced as a metabolic intermediate in several organisms by protein *N*-demethylation and DNA/RNA or metabolite demethylation (Scheme 1).[2] Under physiological conditions, 0.2–0.4 mmol of FA is present in the brain, where it plays a crucial role in memory processing.[3,4]

It is also widely used in many industries, including plastic production, detergents, wood processing and pharmaceuticals.[5,6] At the same time, formaldehyde can be found in the environment as an indoor air pollutant. In particular, the indoor exposure is higher than the outdoor exposure due to the lower air exchange rate. For example, wood-based materials, flooring materials and adhesives[7] commonly found in prefabricated houses release toxic concentrations of FA into the environment over extended periods.[8] At the same time, FA can be found as an atmospheric pollutant. Many natural and human sources of FA can be found in outdoor environments.[9] In fact, FA is produced not only by the decomposition of lignin[10] and isoprene,[11] but also by the ozonolysis of different organic compounds.[12] Also, wood combus-

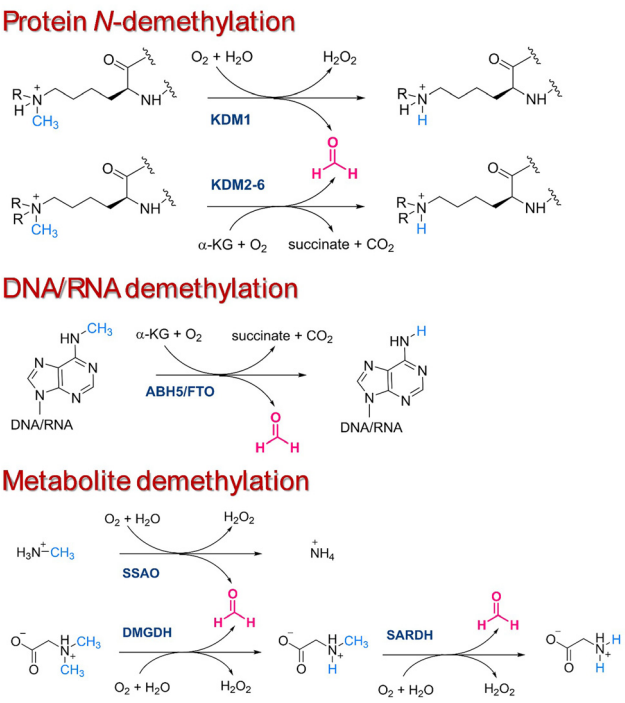

Scheme 1 Some biological pathways that produce FA by enzymatic reactions: α-KG, α-ketoglutarate; KDM, lysine demethylase; SSAO, semicarbazide-sensitive amine oxidase; DMGDH, dimethylglycine dehydrogenase; SARDH, sarcosine dehydrogenase; and FTO, fat mass and obesity-associated protein.

[a]*Department of Chemical Sciences, University of Catania, viale A. Doria 6, 95125, Catania, Italy. E-mail: giuseppe.trusso@unict.it*
[b]*INSTM Udr of Catania, Viale Andrea Doria 6, 95125, Catania, Italy*

tion is the main cause of FA release outdoors.[13] Notably, anthropogenic activity, *i.e.* transport, aircraft and industries, also leads to an increase in the FA concentration in the atmosphere.[14]

From a biological point of view, it is extremely toxic due to the possibility of DNA damage, and it can also cause lachrymation, sneezing, coughing, somnolence and stupor, Alzheimer's disease, and even death in some cases.[15–17] For these reasons, the International Agency for Research on Cancer (IARC) included formaldehyde in the human carcinogen Group I.[18] In fact, FA shows high reactivity towards alcohols, thiols, and carboxylic compounds, leading to toxic effects in the human body.[19] The half-time of FA in a normal environment is one hour, so the indoor FA levels permitted are in the range 0.02–4 ppm, while the allowed outdoor range is 20 ppt–6 ppb.[20]

Taking into account all these considerations, several efforts have been made to detect FA selectively in the gas phase,[21] as well as in foods and other matrices, using different methodologies such as chromatographic and spectroscopic instrumentation[22] and electrochemical,[23] optical and photochemical sensing. Instrumental techniques are preferred in laboratory settings due to their high sensitivity and selectivity. Nevertheless, they have some limitations, because the equipment is often bulky and expensive, and its use requires qualified operators, thus making those methods unsuitable for real-time and *in situ* applications. However, electrochemical methods provide a cheaper and portable tool for environmental analysis. Indeed, they are well known for their fast response time and good sensitivity. However, correct quantification is challenging because electrochemical sensors convert even small non-specific changes into current, thus suffering interferences from other analytes in complex matrices and requiring frequent calibrations.[24] In this regard, optical sensing offers important advantages such as non-invasiveness, high sensitivity, cost-effectiveness and ease of operation.

This review summarizes the developments of FA optical sensing using fluorescent organic compounds. Considering that the last two reviews on this topic date back to 2017[25] and 2021,[26] this review covers both the literature not included in these works and the most recent contributions reported to date. Other recent reviews on FA detection are reported by Roy, Pan *et al.*,[27,28] but they refer to polymeric probes.

Sensing mechanisms of fluorescence detection of FA

In general, fluorescence sensing can be performed *via* two different approaches: covalent and non-covalent, also called "supramolecular", approaches.[29] In both cases, the chemical structure of the sensor contains two main parts: a chromophore and a recognition site (see Scheme 2). The chromophore is the part of the sensor that shows fluorescence emission properties that are modified after the interaction with the target analyte (FA). The monitoring of these changes can be related

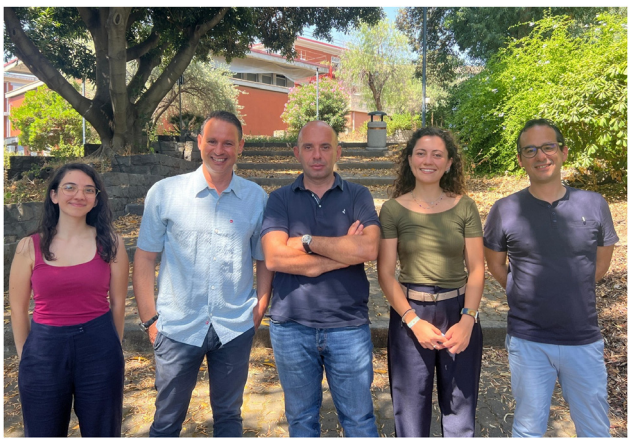

From left to right: Alessia Cavallaro, Andrea Pappalardo, Giuseppe Trusso Sfrazzetto, Rossella Santonocito and Nunzio Tuccitto.

Rossella Santonocito received a Master's Degree in Chemical Sciences (curriculum Organic and Bioorganic Chemistry) in July 2021. She then received a PhD in Chemical Sciences, working on multi-array sensors to detect biomarkers of stress released in extreme environments. Actually, she is a Post-Doc at the University of Catania, working on a new array of devices for human health.

Andrea Pappalardo received a degree in Chemistry and Pharmaceutical Technologies from the University of Catania. Since 2018, he has been an Associate Professor of Organic Chemistry. The research activity is focused on the synthesis of calixarene macrocycles and their use as catalysts in enantioselective epoxidations and receptors in the supramolecular host/guest chemistry.

*Prof. Nunzio Tuccitto received his PhD in Chemistry in 2007. He is currently an Associate Professor of Physical Chemistry at the University of Catania, Italy. He studies the theoretical models governing molecular communication between implantable medical devices, synthesizes molecular messengers based on carbon nanoparticles, and develops bench-top prototypes to test communication. His research activity also focuses on developing nanoparticles for the detection of hazardous gases (*e.g. *Warfare Agents and explosives) and the monitoring of anthropogenic pollutants in the troposphere.*

Alessia Cavallaro received a Master's Degree in Chemistry with 110/110 cum laude*, working on multi-array sensors to detect stress biomarkers. She is currently a PhD student in Chemical Sciences, working on the development of new sensing devices for environmental security.*

Giuseppe Trusso Sfrazzetto received a Master's Degree in Chemistry (Organic and Bioorganic Chemistry, University of Catania) in 2007 and a PhD in Chemical Sciences in 2011. Actually, he is Associate Professor of Organic Chemistry in the Department of Chemical Sciences, in the University of Catania. His research activity focuses on the development of supramolecular sensors for human health and security.

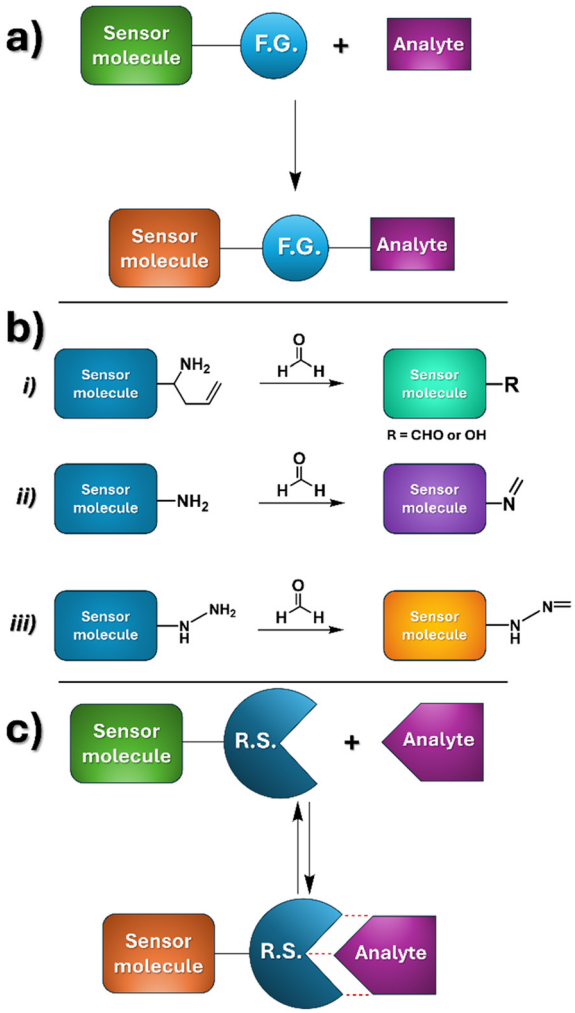

Scheme 2 Sensing of a generic analyte by (a) covalent and (c) supramolecular approaches. (b) Covalent sensing of formaldehyde by (i) the aza-Cope, (ii) the formimine and (iii) the methylenehydrazine reactions.

to the detection of FA, from both qualitative and quantitative (the best-case scenario) points of view. The recognition site is the part of the sensor that interacts with the target analyte. In the case of the covalent approach (Scheme 2a), the recognition site reacts with FA, leading to a new chemical compound, which presents different emission properties (*e.g.* intensity or maximum emission wavelength) compared to the starting sensor. In particular, three main reactions are employed to detect FA until today: (i) the aza-Cope, (ii) the formimine and (iii) the methylenehydrazine reactions (see Scheme 2b).

In the aza-Cope rearrangement reaction, a homoallylamino group reacts with FA, leading to a [3,3]-sigmatropic rearrangement, obtaining a new aldehydic compound with higher emissions with respect to the starting molecule.[30]

In the formimine reaction, FA reacts with an amino group contained in the sensor structure, leading to the formation of a Schiff base. The change in fluorescence is due to a charge or electron transfer mechanism, in which the lone pair on the amino group is involved.[31]

Similarly, a methylenehydrazine reaction is due to the acylation reaction between a hydrazine functional group contained in the sensor and FA.

This approach is the most used in FA detection, but can suffer from some important limitations such as low selectivity, slow reaction time and impossibility to efficiently restore the starting sensor. Otherwise, in the case of a non-covalent approach, the recognition site shows non-covalent interactions with FA, such as hydrogen bonds and dipolar interactions, leading to a supramolecular complex that can be destroyed, recovering the starting sensor (Scheme 2c).[32,33] In addition, if the sensor (in particular, the recognition site) is properly designed, sensing can be highly selective, fast and highly efficient (in terms of binding constant values).[34,35]

FA Sensing *via* aza-Cope mechanism. Zhao *et al.*[36] designed a fluorescent probe (TPE-FA) incorporating an aggregation-induced emission (AIE) fluorophore (tetraphenyl-ethylene) to facilitate rapid detection of gaseous FA *via* a fluorescence "turn-on" mechanism (Fig. 1). Moreover, a portable solid sensor was obtained by soaking a high-performance thin-layer chromatography silica gel plate in a TPE-FA solution, thus achieving sensitive, selective, easy and quantitative detection of FA. TPE-FA reacts with FA *via* 2-aza-Cope sigmatropic rearrangement, increasing its quantum yield from 2.64% (limited by photoinduced electron transfer between electron donor and acceptor groups) to 35.42%. This makes the detection visually discernible to the naked eye. The detection limit of the solid sensor is 0.036 mg m^{-3}, below the air quality guideline threshold for FA (0.1 mg m^{-3}). Compared to solution-based sensors, the AIE-based solid sensor for gaseous FA enables safer and easier use and transport.

Li *et al.*[37] reported a hydrophilic polymeric sensor based on chitosan (HN-Chitosan), which is functionalized with hydrazino-naphthalimide groups, and it was designed for FA detection in aqueous environments. The sensor operates *via* a chemical reaction specifically occurring between FA and the hydrazino-naphthalimide groups, leading to a turn-on fluorescence response from the naphthalimide fluorophores. Unlike precedent sensors, which rely solely on FA-triggered chemical reactions at the molecular level, HN-chitosan employs random coil polymer chains. This design leverages the cooperative binding effect of multiple hydrazino-naphthalimide recognition sites and nearby OH groups, which help to

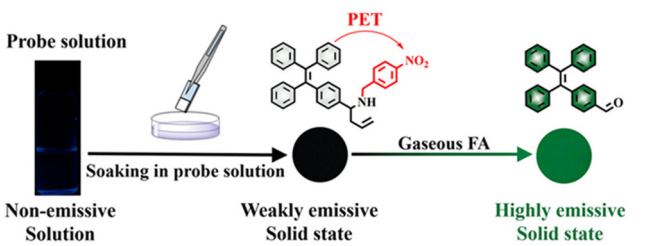

Fig. 1 Preparation of TPE-FA in the solid state and variation in emissions in response to gaseous FA. Reproduced from ref. 36 with permission from the American Chemical Society, copyright 2018.

concentrate low levels of FA around the polymer *via* weak supramolecular interactions: this significantly accelerates the FA-specific reaction, producing an ultra-fast fluorescence response in less than a minute with high sensitivity. HN-chitosan is characterized by photostability, a detection limit of 0.05 ppm and a wide linear detection range between 1 and 100 ppm. Finally, the sensor was successfully tested with real food and water samples.

Yang *et al.*[38] designed a turn-on fluorescent probe (PBD-FA) based on the intramolecular charge transfer (ICT) mechanism, presenting a long wavelength emission (563 nm), adequate for the detection of FA in an aqueous medium and living cells. The probe is made up of two functional parts: a fluorophore which was used as a fluorescence reporter, in particular pyrrolidinyl benzoxadiazole (PBD), and a reaction site chosen to be selectively reactive towards FA, specifically a homoallylamino group (Scheme 3). The homoallylamino reactive group has a poor electron-withdrawing capability, thus making the probe itself not fluorescent. Nevertheless, the presence of FA activates condensation with the reactive moiety, producing an imine intermediate that is converted into an aldehyde derivative through 2-aza-Cope rearrangement followed by hydrolysis. The product showed a remarkable fluorescence, and its ICT efficiency was proven through DFT calculations. Moreover, a good signal was observed in a real sample of living HeLa cells *via* confocal fluorescence microscopy imaging.

Zhou *et al.*[39] designed and synthesized a novel ratiometric fluorescent probe (HBT-FA) based on an aza-Cope reaction, showing high selectivity towards FA in an aqueous solution, serum and air. The probe was obtained starting from a fluorophore, in particular 2-(2-hydroxyphenyl)benzothiazole, and an electron-rich group, which behaves as the reaction site towards FA by 2-aza-Cope rearrangement. Under excitation at 350 nm, the probe HBT-FA shows emission at 462 nm. In the presence of FA, the 2-aza-Cope rearrangement occurs, turning the electron-rich group into an electron-deficient group. This change triggers a pronounced process of intramolecular charge transfer (ICT), resulting in a significant red-shift of the emission band of the probe (λ_{em} = 541 nm), and thus, producing ratiometric signals. The emission ratios (F_{541}/F_{462}) produced a good linearity in the range of 0–30 mM, affording a limit of detection of 0.41 mM. The probe was also tested in air using paper strips soaked into a solution of the probe. Within 1 hour, the test paper over a FA solution turned its colour from blue to yellow, suggesting a future application of HBT-FA for FA detection at the gas phase.

In 2019, Zhai *et al.*[40] developed a new ratiometric fluorescent probe (TP-FA), able to detect FA in aqueous solutions and also in air when loaded on fabric or cotton. The latter exhibited the fastest response to the pollutant compared to the other tests. In fact, as the test cotton was exposed to gaseous FA, a 2-aza-Cope rearrangement occurred between the probe TP-FA and FA, thus changing the colour of the emission from blue to green within 45 min, below the time needed for the test solution and test fabric. Additionally, it provided a visual indication of FA concentration based on the emission colour. This variation can be explained through the combination of intramolecular charge transfer (ICT) and aggregation-induced emission (AIE) effects. This study marks the first application of fabric and cotton for gaseous FA detection.

Yunxu *et al.*[41] reported on the selective recognition of FA over other carbonyl compounds by a novel fluorescent ZIF-90 MOF material (ZIF-90-LW). This material, characterised by FT-IR spectroscopy, X-ray diffraction and SEM, shows a fluorescence turn-on signal due to a 2-aza-Cope rearrangement mechanism, upon addition of increasing amounts of FA (Fig. 2 (top)). The authors found a good linearity relationship (R^2 = 0.9979) by fitting the fluorescence intensity in the range of 0 to 25 mM of FA, and a detection limit of 2.3 mM. The high selectivity of ZIF-90-LW toward FA was proved in the presence of different analytes, comprising several aldehydes, acetone, glucose and H_2O_2. Moreover, a fluorescence test paper of ZIF-90-LW was constructed to detect FA in the gas

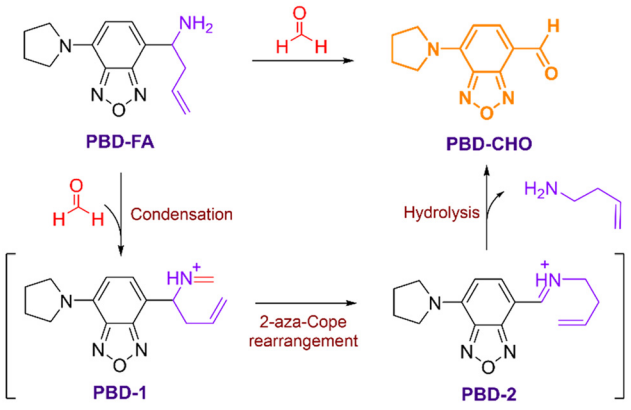

Scheme 3 Turn-on sensing mechanism of the fluorescent probe PBD-FA.

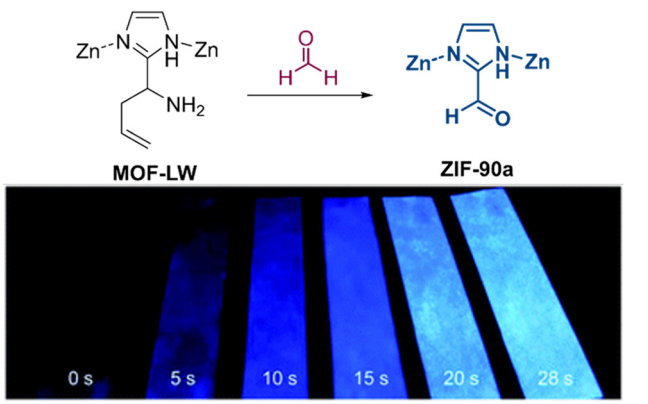

Fig. 2 (Top) Design showing the response of ZIF-90-LW towards FA and (bottom) strip test in the presence of FA under 365 nm at different times. Adapted from ref. 41 with permission from the Royal Society of Chemistry, copyright 2020.

phase, showing a fast response and paving the way for the monitoring of FA in the environment (Fig. 2 (bottom)).

In 2021, Zheng *et al.*[42] reported a fluorescent silica aerogel designed for the detection of gaseous FA. The fluorescent aerogel exhibits high sensitivity, selectivity, stability and a LOD of 110 ppm. Its sensing mechanism relies on an aza-Cope rearrangement reaction within a fluorescent probe. The binding of FA induces changes in fluorescence emission, enabling precise detection. Fluorescent probes are chemically bonded to the aerogel network, ensuring durability and stability of the sensing performance. Characterisation of the aerogel revealed a porosity exceeding 95.9% and a specific surface area of 779 $m^2\ g^{-1}$. Its mesoporous structure enhances gas absorption, a property confirmed through SEM imaging and nitrogen adsorption analysis. In controlled testing environments, FA gas was introduced, and the fluorescent aerogel demonstrated rapid interaction and a distinct fluorescence change. The material also displayed excellent selectivity, effectively detecting FA in the presence of other volatile organic compounds, including toluene, ammonia, and carbon dioxide, with minimal interference.

Ai *et al.*[43] introduced a fluorescent probe based on the 2-aza-Cope reaction for relevant application under several conditions including food industry (vegetables, dairy products, meat, fish, mushroom, and legumes). After the reaction with FA, the solution colour of the probe changes from blue to green under 365 nm UV light, and the fluorescence intensity is significantly enhanced. The authors also prepared electrostatically spun fibre membranes by mixing the fluorescent probe with PVDF-HFP for the selective detection of FA soil, in living cells and zebrafish.

Chen *et al.*[44] introduced an innovative paper-based material combining polyethyleneimine (PEI) and a highly sensitive fluorescent probe (FP) for the simultaneous detection and removal of FA (Fig. 3). The fluorescent probe exhibits a bright blue fluorescence emission at 450 nm. When exposed to FA, it decreases by approximately 80%, while a new fluorescence signal emerges at 540 nm, increasing with higher FA concentrations. The ratiometric fluorescence signal (F_{540}/F_{450}) enhances over 100-fold, enabling precise detection. The detection process demonstrates a strong linear relationship between fluorescence intensity changes and formaldehyde concentration with a detection limit calculated to be 0.46 μM, ensuring high sensitivity. Since fluorescence changes are visually striking, transitioning from bright-blue to yellow-green under UV light allows naked-eye detection. The system's selectivity was tested against a variety of potential interfering substances, including common aldehydes, organic compounds, metal ions, and anions. FP showed a significant fluorescence enhancement only in the presence of FA, with minimal interference from other substances. The paper-based material exhibits exceptional FA removal efficiency.

FA sensing by imine mechanism. In 2018, a bio-compatible fluorophore, 7-nitrobenz-2-oxa-1,3-diazole (NBD), was easily tagged with amino-ethyl piperazine by Gangopadhyay *et al.*,[45] forming a conjugate (NPC): the obtained sensor was successfully employed for the fluorimetric detection of gaseous FA. The sensing mechanism relies on the inhibition of photo-induced electron transfer (PET) due to the formation of the Schiff base formimine, when the probe NPC reacts with FA (Scheme 4). The sensor is highly selective and robust, with a rapid response time (2 min) and a low limit of detection (84 nM). The probe was then employed to fabricate a solid sensor for the detection of FA emissions coming from plywood, using TLC test strips as solid supports. The results demonstrated that the sensor has a practical applicability in the gas phase for the detection of FA emissions from wooden furniture, so it represents a promising candidate for the creation of affordable and portable sensing kits. Moreover, the sensor was also successfully applied in cellular imaging, demonstrating its potential for further studies aimed at monitoring the concentration of FA in living cells.

Lin *et al.*[46] described FA detection by fluorescent CD@SiO_2-NH_2 nanoparticles containing carbon dots (CDs) within silica spheres. The addition of Ag^+ ions to the amino-functionalized nanoparticles results in the chelation of silver ions, and the formation of the fluorescent probe CD@SiO_2-NH_2-Ag^+. The exposure of CD@SiO_2-NH_2-Ag^+ to FA triggered the *in situ* growth of AgNPs, due to the reduction of the silver-ammonia complex. These AgNPs present a strong enhancement of fluorescence intensity with respect to CD@SiO_2-NH_2-Ag^+, leading to a clear change in color due to a Metal-enhanced fluorescence (MEF) mechanism. An assay was developed considering that an increase in FA concentration corresponds to an

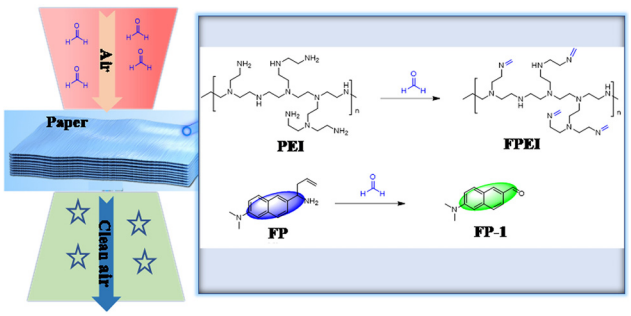

Fig. 3 Mechanisms involved in multifunctional fluorescent materials for FA detection and removal. Reproduced from ref. 44 with permission from Elsevier, copyright 2025.

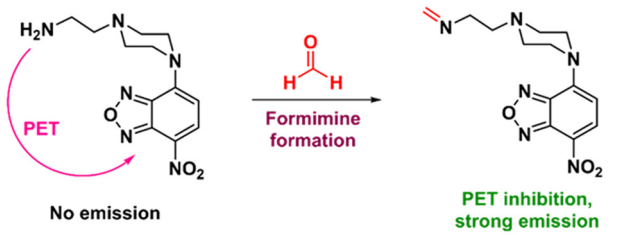

Scheme 4 Proposed mechanism for sensing FA with probe NPC.

increase in fluorescence enhancement factor. Then, a linear response in the range of 1–50 μM of FA was determined (R^2 = 0.99), with an LOD of 0.1 μM. Notably, the CD@SiO_2-NH_2-Ag^+ probe was loaded onto a nano-sponge material for gaseous FA detection. The emission intensity upon formaldehyde exposure is strongly enhanced, showing a linear relationship in the range of 10 ppb to 1 ppm of formaldehyde gas concentration, and a limit of detection of 3 ppb. Selectivity tests with other carbonyl interferents revealed that these compounds cause fluorescence enhancement, although half that of FA.

Bej *et al.*[47] developed two luminescent porous d^{10}-MOFs, namely CMERI-1 and CMERI-2, featuring amine-functionalized building units for FA detection in water, characterised by easy syntheses. CMERI-1 demonstrates superior sensitivity with a response time of just one minute due to easy imine formation, whereas CMERI-2 requires five minutes. The fluorescence "turn-on" effect is attributed to the inhibition of the PET process (Fig. 4). The detection limits for FA in aqueous solutions are 0.62 μM for CMERI-1 and 1.39 μM for CMERI-2. Additionally, a MOF-based hydrogel membrane was created to detect FA in the vapor phase. These porous hybrid materials show great potential for on-site FA detection in both aqueous and vapor phases, making them suitable for real-world applications in food and water analysis. Furthermore, these materials exhibit remarkable selectivity for FA over other aldehydes.

Tachapermpon *et al.*[48] developed a FA detection system using nitrogen-doped carbon dots (N-doped CDs). The system achieves a limit of detection of 22 μg L^{-1}. The sensing mechanism relies on a fluorescence "turn-off" response, where the interaction between the amino groups of N-doped CDs and the carbonyl group of FA causes fluorescence quenching. The CDs are synthesised hydrothermally from citric acid and ethylenediamine, resulting in highly luminous, biocompatible nanoparticles with strong UV fluorescence.

FA exposure tests involved controlled environments where ornamental plants treated with N-doped CDs were exposed to FA for one hour. The response was linear across FA concentrations from 36 to 270 μg L^{-1}, ensuring accurate quantification. When sprayed onto *Fittonia albivenis* (Nerve Plant), the CDs allow for visible FA detection *via* fluorescence quenching under UV light. This system demonstrates excellent selectivity for FA over other volatile organic compounds (VOCs) such as acetone and tetrahydrofuran. This phytosensor provides a cost-effective, visual approach for monitoring FA pollution, making it ideal for indoor air quality applications. Its biocompatibility and ease of use suggest potential for broader environmental and agricultural uses.

Tan *et al.*[49] synthesized three different fluorescein probes for the selective detection of FA in polluted water. The probes are 2-(phenylethynyl)aniline, 3-(phenylethynyl)aniline, and 4-(phenylethynyl)aniline. The mechanism of action of sensing is based on photoinduced electron transfer between the N=CH_2 group and diphenylacetylene. The authors reported the relationship between amino substitution position and FA detection performance. The probes showed increased fluorescence at 508 nm when excited at 370 nm. They showed selectivity towards biologically relevant analytes, including reactive carbonyl species, acid and alcohol species and cations in water. The authors claim an LOD of 0.75 μM with a linear dynamic range up to 1000 μM.

Ma *et al.*[50] reported the exploitation of the fluorescence properties of sodium ligninsulfonate-derived carbon dots (CDs) for the detection of FA with an LOD of 79 nM and a linear dynamic range of up to 50 μM (Fig. 5). A visual on-site detection of indoor FA gas is realized by using the CD-droplet detection system. This system, based on polyvinyl alcohol and CDs, was developed for the effective detection of indoor FA gas. For this detection system, one simply brushes the PVA/CD gel onto a clean solid surface to form the droplet. With the advantages of low cost, simple preparation, rapid response and visual detection process, the discovery is of relevant interest.

Bai *et al.*[51] developed a ratiometric fluorescence sensing system using ethylenediamine-functionalized and europium-doped UiO-66 (EDA-Eu^{3+}@UiO-66) for the selective and sensitive detection of FA. This system exploits the antenna effect characteristic of lanthanide elements, where the energy absorbed by the UiO-66 framework is efficiently transferred to Eu^{3+} ions, resulting in their characteristic fluorescence emission. The detection mechanism is based on the interaction of FA with amine groups on the EDA-Eu^{3+}@UiO-66 surface *via* aldehyde-amine condensation, which reduces the efficiency of energy transfer and causes fluorescence quenching. To evalu-

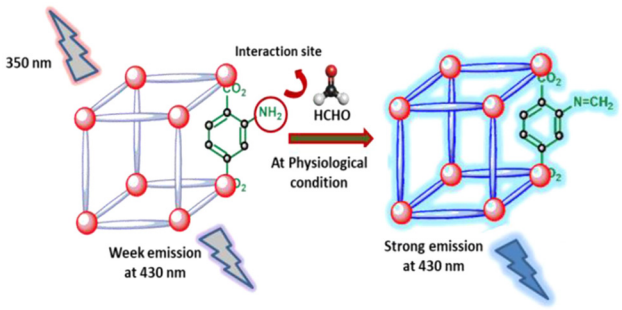

Fig. 4 "Turn-On" sensing of FA by the d10-MOF (CMERI-1) under physiological conditions. Reproduced from ref. 47 with permission from the American Chemical Society, copyright 2021.

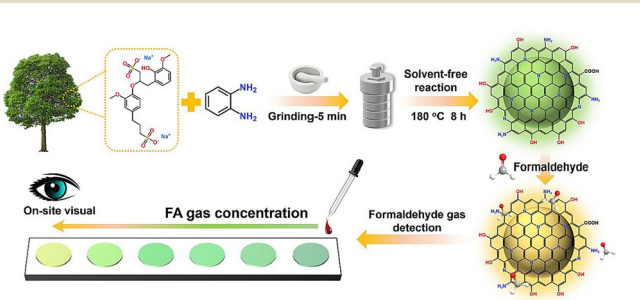

Fig. 5 Synthesis of nanoparticles and formaldehyde sensing. Reproduced from ref. 50 with permission from Elsevier, copyright 2024.

ate the system's performance, a dispersion of EDA-Eu^{3+}@UiO-66 in water was prepared and tested with varying concentrations of VOCs, including FA. The fluorescence measurements, conducted with an excitation wavelength of 280 nm, showed a distinct quenching effect in the presence of FA. The detection limit for FA in solution was determined to be 0.38 mg L^{-1}, indicating the high sensitivity of the probe. In addition to liquid-phase detection, the study demonstrated the system's capability to detect FA vapor. Filter paper strips coated with EDA-Eu^{3+}@UiO-66 were exposed to various concentrations of FA vapor in a sealed chamber. A noticeable quenching of fluorescence was observed, validating the system's ability to function effectively in gaseous environments.

Wang *et al.*[52] developed a fluorescent probe, called probe X, based on 1,8-naphthalene dicarboxylic anhydride as a fluorophore, bearing a hydrazine as an FA recognition site. The mechanism of FA detection lies in the inhibition of the PET process between the naphthalimide derivative and the hydrazine group, resulting in an enhancement of the fluorescence. The probe showed a good optical response in a linear range of 1–4 mM and a rapid response time of 2 minutes. Moreover, probe X exhibited biocompatibility, minimal toxicity and excellent membrane permeability, giving the possibility to employ it for fluorescence imaging in living cells.

Roy *et al.*[53] reported the development of a naphthalimide-conjugated polymeric fluorescent probe (DCP5) for the selective detection of FA in both aqueous and vapor phases. The sensing mechanism relies on the reaction between FA and amino-functionalized naphthalimide pendants. This reaction is enhanced by the synergistic effects of multiple recognition sites *via* supramolecular interaction with the polymer coil. Following the reaction, the PET process is suppressed, resulting in rapid "turn-on" green fluorescence irradiation at 365 nm, with a response time <1 min and an LOD of 1.36 nM. For vapor-phase detection, the polymer was covalently immobilized onto filter paper *via* UV-induced crosslinking, facilitated by benzophenone moieties in the polymer backbone. The resulting paper strip shows visible fluorescence changes upon exposure to FA vapor, providing a promising platform for *in situ* detection. Moreover, the FA–polymer adduct (DCP5-FA) can be reversed, allowing regeneration of the sensor.

FA sensing by methylenehydrazine mechanism. Zang *et al.*[54] proposed a fluorescence-based system developed by modifying the surface of CdTe/CdS QDs with an organic ligand, *i.e.* 3-(6-hydrazinyl-1,3-dioxo-benzoisoquinolinyl)propanoic acid (HBQP) (Scheme 5). This ligand was introduced on QDs *via* a surface-ligand exchange process. When FA interacts with the HBQP-coated QDs, it frees fluorescent species with emission at 540 nm, while the QDs lose their fluorescence at 666 nm, thus achieving a dual detection mode. This system can detect FA in both liquid and gas forms using a solid sensor made of cellulose paper. The linear range within the fluorescence intensity changes in proportion to FA concentration is between 1 and 28 μM. The calculated LOD is 0.49 μM, which meets the standards set by environmental authorities.

Scheme 5 Fluorescence quenching of QD-HBQP and fluorescence appearance of HBPQ after FA addition.

Lin *et al.*[55] proposed a new method for ultrasensitive FA detection in solution and gas using a catalyst-preplaced sensor based on a pillar[5]arene functionalized with two thioacetylhydrazine moieties (DP5J). The design of the sensor involved different functional parts: hydrazine groups were incorporated to serve as recognition sites for reaction with FA and as self-assembly sites *via* hydrogen bonding; the pillar[5]arene was used as an aggregation-induced emission (AIE) fluorophore and as a π–π stacking site. Using the catalyst $(CF_3SO_3)_2Bi$ to enhance the recognition efficiency, the probe DP5J could detect FA through a turn-on fluorescence response driven by an AIE mechanism. The detection of FA occurred within 7.5 s, and the detection limit is 3.27 nM. Moreover, the sensor demonstrated high selectivity for FA, as evidenced by the lack of interference from other aldehydes during the detection process. Additionally, the catalyst preplaced sensor (DP5J-Bi) was employed to create a test kit for FA sensing, using a silica gel plate as support to load the solution. The test kit demonstrated high sensitivity, which made it suitable to detect FA in solution or in gas.

Lately, Suhua *et al.*[56] reported a fluorescence enhancement probe (FAP) containing 7-nitrobenzo-2-oxa-1,3-diazolyl (NBD) dye as the fluorophore, which shows a turn-on fluorescence response to FA detection with high selectivity and sensitivity. The FAP chemoprobe was easily prepared by a reaction between hydrazine and NBD chloride. The obtained FAP displays weak fluorescence due to the photo-induced electron transfer (PET) process involving the hydrazine moiety. The addition of formaldehyde in acidic pH leads to a methylenehydrazine Schiff base derivative, resulting in the suppression of PET and, consequently, increasing fluorescence. The authors reported that under strong acidic conditions (pH = 2.8), the FAP showed a stronger fluorescence intensity (30 times) in the presence of FA, linearly responding in a range of 0.015–0.8 mg L^{-1}. Selectivity tests were performed in the presence of an excess of various interferents (acetone, acetaldehyde, methanol, ascorbic acid, H_2O_2, and Na_2S), highlighting that only acetaldehyde noticeably affects the FA-induced fluorescence enhancement.

Cao *et al.*[57] reported a fluorescent Schiff base probe based on 2,5-dihydroxy-*p*-benzenedicarbonamide (DTH), able to detect FA and acetaldehyde in external environments and cells. Upon excitation at 385 nm, DTH shows a maximum fluorescence emission band at 508 nm, and a low fluorescence quantum yield (Φ_f = 0.027 ± 0.001), mainly due to a PET process or an ICT process. The addition of FA or acetaldehyde to DTH revealed a different behavior of this probe. DTH has

proven to be a ratiometric probe for FA, showing a decrease in the intensity of the maximum emission peak at 508 nm and a red shift to 534 nm with an increase in intensity emission, due to the formation of the C=N double bond (Φ_f = 0.055). Conversely, the addition of acetaldehyde to DTH produces a slight red shift (7 nm) with a strong enhancement of the luminescence emission intensity (Φ_f = 0.122), due to the presence of the electron-donating methyl group that affects the PET process (Scheme 6).

Furthermore, detection limits of 0.29 μM with a linear response in the range of 0–0.02 mM and 0.26 μM with a linear response in the range of 0–0.035 mM were found for FA and acetaldehyde, respectively. Selectivity tests towards FA and acetaldehyde were conducted with aldehydes (propylaldehyde, *p*-nitrobenzaldehyde, *p*-methoxy benzaldehyde) and other compounds (hydroquinone, glucose, NaHS and H_2O_2), highlighting that no significant red shift of the emission wavelength was observed with selected interferents. Finally, since DTH was found to be non-toxic, its use in detecting the presence of FA and acetaldehyde in HeLa cells was investigated.

In 2021, Wang *et al.*[58] reported a fluorescent sensing film for the detection of FA and acetaldehyde, based on a naphthylamide derivative, namely 6-hydrazineyl-2-(2-methoxyethyl)-1*H*-benzo[de]isoquinoline-1,3(2*H*)-dione (HBD). This derivative was infiltrated in SiO_2 inverse opal photonic crystals. The detection mechanism lies in the nucleophilic addition between the amine group of the naphthalimide derivative and the aldehydes, leading to a strong fluorescence emission at 550 nm. The emission is significantly enhanced due to the slow photon effect of the photonic crystals, where the emission wavelength aligns with the stopband edge, thus obtaining detection limits of 10.6 nM and 7.3 nM for FA and acetaldehyde, respectively, with a response time of 1 minute. Additionally, the nucleophilic addition product can be easily hydrolysed in an acidic aqueous solution, thus achieving reversibility of the sensor. This sensor was employed to detect FA and acetaldehyde in real samples, such as aquatic products and living cells.

In 2022, Ye *et al.*[59] developed a dual-channel sensor, Nap-NH_2, able to detect FA and phosgene with exceptional sensitivity and selectivity. The sensor achieves limits of detection of 62 nM for FA and 23 nM for phosgene. The sensing mechanism relies on the hydrazine group in Nap-NH_2 undergoing distinct reactions with the two analytes. Interaction with FA forms a hydrazone group, resulting in fluorescence enhancement at 551 nm, while reaction with phosgene produces an amide, causing fluorescence at 487 nm. Nap-NH_2 is synthesised from 4-chloro-1,8-naphthalic anhydride and hydrazine, incorporating strong ICT and PET effects for efficient signal generation. The sensor's fluorescence response is rapid, stabilising within 12 minutes for FA and just 2 minutes for phosgene. The detection modes exhibit excellent linearity in the range of 0–80 μM for FA and 0–150 μM for phosgene. Nap-NH_2 demonstrates high selectivity, effectively distinguishing FA and phosgene from other aldehydes and reactive compounds with minimal interference. To facilitate practical applications, portable test strips based on Nap-NH_2 were developed for on-site detection. Smartphone-based fluorescence imaging further supports remote monitoring, making the system economical, portable, and suitable for field applications.

Cao *et al.*[60] reported the synthesis of a fluorescent sensor, bearing quinolimide as a fluorophore and hydrazine as a reaction site for the covalent recognition of FA with a turn-on mechanism of fluorescence (Fig. 6). Linear response towards FA was confirmed in the range of 0–180 μM, with a calculated LOD of 1.7 μM in a methanol-PBS buffer. The emission turn-on has been rationalized by the PET mechanism upon the covalent reaction of FA with the amino group of the sensor, confirmed by DFT calculations. Selectivity was demonstrated

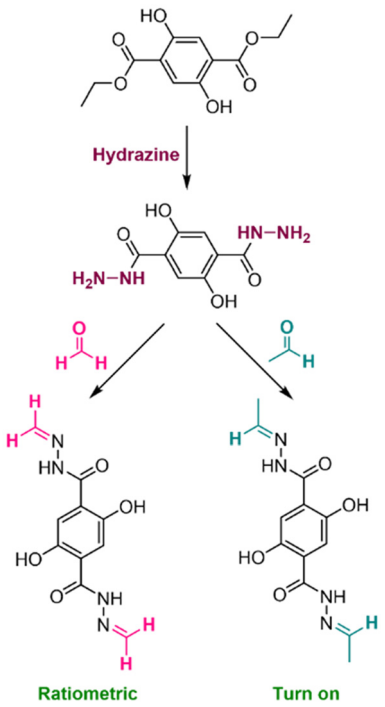

Scheme 6 Synthesis of DTH and fluorescence changes with FA and acetaldehyde.

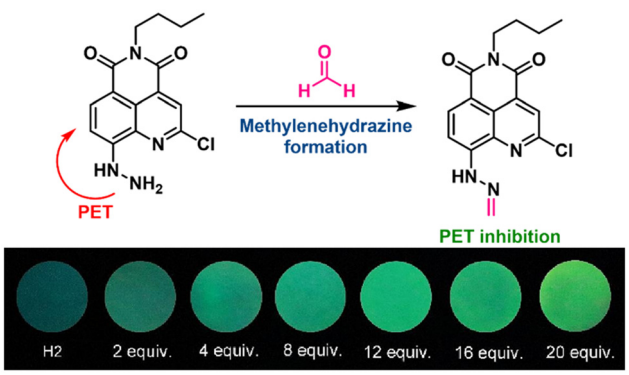

Fig. 6 Sensing mechanism and real image photos. Adapted from ref. 60 with permission from Elsevier, copyright 2023.

in competition mode using different other interferents. This sensor was also used in solid phase by a strip test, and into yeast cells treated with an excess of FA, supporting the possibility to use this sensor for real-time applications.

In 2025, Ye *et al.*[61] designed a fluorescent probe named OPTY, derived from 8-hydrazine-boron-dipyrromethene (BODIPY), for the dual detection of FA and nitrite (NO_2^-) in food. OPTY reacts with FA *via* aldimine condensation to emit blue fluorescence (465 nm), and with NO_2^- *via* intramolecular cyclization to produce green fluorescence (510–520 nm). The probe demonstrates high sensitivity, selectivity, strong signal-to-noise ratio, and low detection limits (26.5 nM for FA and 20.8 nM for NO_2^-). To facilitate *in situ* analysis, OPTY was incorporated into cellulose paper strips and integrated with a smartphone to create a portable sensing platform. This system allows easy, rapid, on-site, visual, and quantitative detection of FA and NO_2^- in food by analysing RGB values from the fluorescent chips under UV light. The platform showed excellent performances in real samples, including meat and seafood, achieving recovery rates of FA between 93.5% and 102.4%.

Pan *et al.*[62] reported a study presenting a water-soluble, naphthalimide-based fluorescent block copolymer (BCP2-N) for selective FA detection in aqueous solutions. The probe features hydrazine side chains, linked with post-polymerization modification, that react with FA *via* an addition–elimination mechanism to form a hydrazone. This reaction disrupts the internal PET process, leading to a distinct green turn-on fluorescence. The formation of the hydrazone and the sensing mechanism were validated through ESI-MS analysis and supported by DFT calculations, respectively. The polymeric probe BCP2-N exhibits excellent sensitivity, detecting FA with an LOD of 1.7 μM, with a five-fold fluorescence increase observed within 10 minutes upon FA exposure. The polymer also demonstrates strong selectivity toward FA over other analytes, combined with excellent water solubility and photostability, thanks to its poly(*N*,*N*-dimethyl acrylamide) (PDMA) block copolymer structure. Despite all these advantages, the probe is able to perform only in aqueous media, because it is not fluorescent in the solid state.

Wang *et al.*[63] synthesised a turn-on fluorescent probe, named W-1a, for the sensitive and selective FA detection in both environmental and biological contexts. The probe is based on a trifluoromethyl quinoline derivative as the fluorophore and a hydrazine moiety, which acts as the reactive site for FA. Upon reaction with FA, fluorescence is restored, enabling quantitative detection with an LOD of 0.91 μM and a response time of approximately 13 minutes. W-1a exhibits high selectivity and stability under physiological pH conditions and in the presence of common interfering substances, such as ions and other aldehydes. These characteristics, united to excellent biocompatibility and low cytotoxicity, make the probe W-1a suitable for live-cell imaging of endogenous and exogenous FA. Practical applications were also validated, with successful FA detection in indoor decorative materials and seafood products, showing high recovery rates.

FA sensing by other mechanisms. Martínez-Aquino *et al.*[64] developed a novel environment-friendly, selective and sensitive sensor, which involves natural compounds, for the detection of FA. In particular, the components of the probe are dopamine, glycine and sucrose and the FA sensing mechanism involves the Pictet–Spengler reaction between primary catecholamines and FA. This passage is then followed by the dehydrogenation of the tetrahydroisoquinoline, to visualize biogenic monoamines through fluorescence microscopy. The probe can detect FA either in aqueous solution or in gas phase: in the first case, the presence of the pollutant can be identified through both colorimetric and fluorescence emission changes, while the second case requires the preparation of test strips with silica gel plates for the colorimetric detection of FA, which can be observed with the naked eye. The obtained supported probe is safe and easy to use. The limit of detection in solution is 0.24 nM, while for the gas phase, the detection limits for 30-minute STEL (Short-Term Exposure Limit) and 10-hour TWA (Time-Weighted Average) are 0.7 ppm and 0.4 ppm, respectively, assessed using the image-analysis software.

In 2021, Li *et al.*[65] reported the development of an FA sensor based on self-assembled monolayers (SAMs) of oxidised thiophene derivatives (Fig. 7). The sensing mechanism relies on the ability of 3T to oxidise under UV light in the presence of oxygen, forming non-fluorescent carbonyl groups. When FA interacts with these groups, a blue-shifted fluorescence is restored, allowing for sensitive detection. The sensor demonstrates high sensitivity, with the ability to detect FA concentrations below 1 ppm. It also exhibits excellent stability and selectivity, making it a reliable tool for FA detection in various environments.

Fang *et al.*[66] reported the development of a supramolecular organic framework (HNU-44) for highly sensitive and selective FA detection in both liquid and gaseous phases. This material demonstrates remarkable performances, significantly outperforming many current FA sensors. HNU-44 achieves a limit of detection as low as 27.41 ppb in water and 2.61 ppb in gas. Its dual sensing mechanism allows it to exhibit fluorescence enhancement towards aqueous FA due to restricted benzene rotation, while with gaseous FA, fluorescence quenching occurs as hydrogen bond activation induces intramolecular rotation. The framework is synthesised *via* the self-assembly of (*Z*)-4,4′-(1,2-diphenylethene-1,2-diyl)dibenzoic acid through hydrogen bonding and π–π interactions. This design endows HNU-44 with exceptional stability in aqueous environments

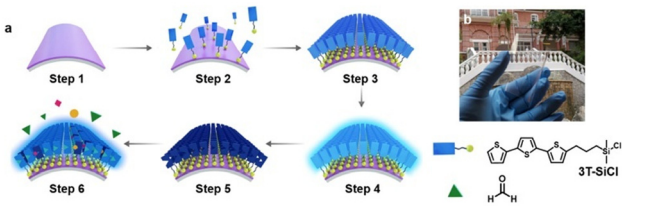

Fig. 7 (a) Schematic of the steps involved in SAM sensor development. (b) Real image of the flexible sensor. Reproduced from ref. 65 with permission from the American Chemical Society, copyright 2021.

across a wide pH range (1–10) and thermal resistance up to 385 °C. HNU-44 exhibits excellent selectivity for FA, with minimal interference from other volatile organic compounds, metal ions, or anions in either liquid or gaseous phases. This selectivity, combined with its high sensitivity, makes it a robust candidate for real-world applications.

Yu *et al.*[67] developed a triangular macrocycle sensor (S1) able to detect FA in aqueous solutions with high sensitivity and selectivity. The sensor achieves a low limit of detection of 22.5 ppb. The sensing mechanism is based on a reversible *N*-hydroxymethylation reaction involving the imidazole groups in the macrocycle, which induces a fluorescence colour change from yellow to green-yellow upon FA binding (Fig. 8). The macrocycle, assembled using imidazole-based ligands (L1) coordinated with Zn^{2+} ions, provides active binding sites for FA and enables fluorescence-based detection. The reaction occurs rapidly under mild conditions, with visual detection achievable within minutes at room temperature. Fluorescence intensity increases linearly with FA concentration over the range of 0.61–8.14 μM. The sensor exhibits excellent selectivity for FA, with negligible interference from other aldehydes and organic compounds. Its reusability is another key advantage, as absorbed FA can be released through heating, allowing for multiple detection cycles.

Wei *et al.*[68] developed a highly sensitive fluorescent sensor based on 1*H*-[1,2,3]triazole[4,5-*b*]phenazine (PHTA) for FA detection. The sensor achieves an impressive limit of detection of 1.55×10^{-8} mol L^{-1} in DMSO solutions. The detection mechanism involves a nucleophilic addition reaction between FA and PHTA, causing a visible fluorescence shift from orange-red to yellow. PHTA, synthesised from phenazine derivatives, boasts a high fluorescence quantum yield, photochemical stability, and strong FA interaction. The sensor delivers rapid detection, reaching equilibrium within 10 minutes. It exhibits linear fluorescence intensity ratio changes (F_{510}/F_{640}) over FA concentrations ranging from 0.48 to 0.92 mM. PHTA demonstrates excellent selectivity, showing minimal interference from other VOCs. A silica-gel-based solid-state sensor was also developed, enabling FA detection in both gaseous and liquid environments, including applications in food samples such as meat. This portable, cost-effective probe is suitable for repeated use, as it can be thermally regenerated. Its combination of high sensitivity, rapid response, and practicality makes it an ideal candidate for environmental monitoring and food safety applications.

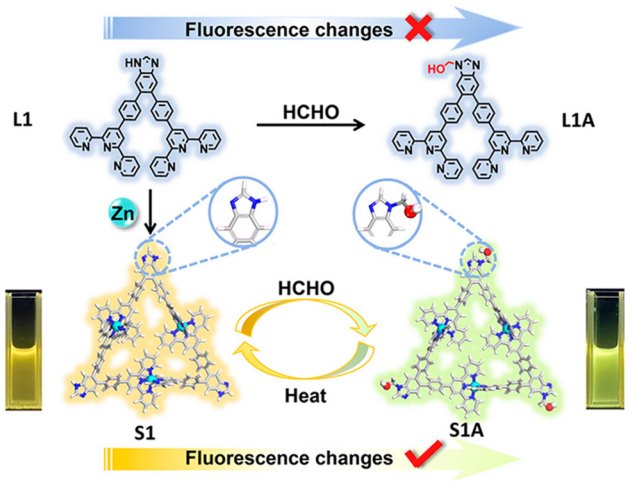

Fig. 8 Fluorescence changes of ligands L1 and S1 with the dropwise addition of formaldehyde. Reproduced from ref. 67 with permission from the American Chemical Society, copyright 2022.

Del Mar Darder *et al.*[69] reported FA sensing using a colorimetric probe based on the evanescent wave absorption due to the interaction of the analyte with Leuco-Fuchsin onto a plastic optical fiber. They used polymethyl methacrylate as an optical waveguide, covered with a Nafion® polymer. In particular, under acidic conditions, Leuco-Fuchsin reacts with FA leading to a violet product, with a maximum absorption at 575 nm, in 15 minutes. The limit of detection of 0.02 ppm, close to the limit of quantification (0.025 ppm) and a linear range of 0.03–5.5 ppm, was calculated. Selectivity was tested with other aldehydes such as benzaldehyde and acetaldehyde, as well as with acetone and methanol in large excess with respect to FA. This system was tested in real field, in particular in industrial paper impregnation processes.

Li *et al.*[70] reported the fabrication of multicolour carbon dots starting from lignin, able to detect FA by visual method. They started from lignin due to the high aromatic rings contained in its structure, ideal for the preparation of carbon dots. The authors obtained different carbon dots, in particular, blue-, cyan- and green-emitting carbon dots, tuning the amount of HCl (as a depolymerization agent), funding the blue emitting carbon dots ideal for FA detection. Sensing was performed under sunlight, showing the formation of a turbid solution with FA concentrations above 0.4 mg L^{-1}. However, with fluorometric method, performances are higher, leading to an LOD of 7.4 μg L^{-1}, a linear range from 0 to 1 mg L^{-1} following a progressive quenching of the emission of the carbon dots. In addition, selectivity was tested with metal cations.

Hou *et al.*[71] described the realization of an indirect FA sensing, exploiting the "on–off–on" emission mechanism due to fluorescence inner-filter effect (IFE) of glutathione-doped CdTe carbon dots and FA, in the presence of $KMnO_4$. IFE is due to the combination of GSH-CdTe and $KMnO_4$, leading a quenching of the emission of carbon dots. In the presence of FA, reaction with $KMnO_4$ occurs, restoring the emission of carbon dots. This reaction occurs in 2 minutes, with a concentration of $KMnO_4$ of 5 μmol L^{-1}, a linear detection range of FA of 0–80 μmol L^{-1} and an LOD of 9.33 nmol L^{-1}. Selectivity with other aldehydes, cations and anions confirms the ability of this sensor in the FA detection.

Liao *et al.*[72] reported a turn-on fluorescent sensor, able to detect FA in gas by turn-on of the emission (Fig. 9). The authors used a porous cellulose plate as a solid support, functionalized with a perylene diimide (PDI) chromophore, bearing a hydroxylamine sulfuric acid salt. In the presence of FA, reaction with the hydroxylamine sulfuric acid salt occurs

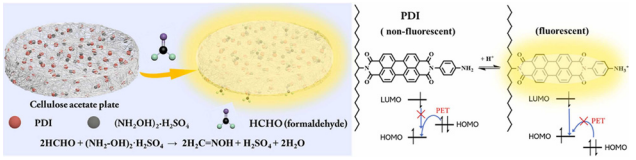

Fig. 9 Formaldehyde sensing mechanism using a functionalized cellulose acetate plate. Reproduced from ref. 72 with permission from Elsevier, copyright 2023.

in 20 minutes, leading to the protonated form of PDI showing higher fluorescence than the initial form. This device shows an LOD of 3.7 ppb, in the linear concentration range of 0–900 ppb of FA. Selectivity was studied with alcohols, hydrocarbons and ammonia.

Fan *et al.*[73] recently reported a method for FA detection in children's toys. In particular, they developed a hybrid system containing a fluorescent whitening agent, potassium dichromate and sulfuric acid that was able to detect FA by fluorescence emission (*via* off-on mechanism) and visual mode (Fig. 10). The internal filtration effect due to the presence of dichromate leads to the quenching of the emission, which is restored in the presence of FA after the reduction of dichromate to Cr^{3+} in *ca.* 25 minutes. Detection limits, by fluorescence and visual methods, are 2.03 and 85.5 mg L^{-1}, respectively. Several interferents were tested, including aldehydes and inorganic salts. This method has been evaluated for water and children's toys analysis, obtaining good recovery values.

Zhu *et al.*[74] synthesized a probe based on a metal–organic framework of europium. It shows fluorescence in the visible region when excited in the ultraviolet region around 360 nm. The authors report an LOD of 194 μM with a dynamic linear range between 0.1 μM and 1 μM. The selectivity of the probe is poor, as it is also sensitive to other substances, in particular Hg^{2+} and Cd^{2+} ions. The probe has also been shown to work on filter paper to detect contaminated solutions.

Cadeado *et al.*[75] proposed an optical technique to detect FA in milk, combining reflectance and fluorescence measurements to improve sensitivity. The approach is based on the Hantzsch reaction between FA and acetylacetone, forming 3,5-diacetyl-1,4-dihydrolutidine (DDL), the optical properties of which can be observed by reflectance at 415 nm and fluorescence at 515 nm. Using a multi-channel spectrometer and an IoT-enabled sensor, the method achieved detection limits of 0.027 mg L^{-1} (reflectance) and 0.030 mg L^{-1} (fluorescence), with linear responses in the 0.1–4 mg L^{-1} and 0.1–3 mg L^{-1} ranges, respectively, using only few microliters of sample. FA concentrations in milk samples were successfully measured, showing a 60% decrease in FA content after thermal treatment at 70 °C for 20 minutes. This is the first reported use of an IoT-based sensor capable of simultaneous fluorimetric and spectrophotometric FA detection. Validation across various milk types (UHT, skimmed, pasteurized, and fortified samples) confirmed its accuracy and reliability. Furthermore, the entire device, featuring a 3D-printed case, Arduino board, sensor, and wiring, was assembled for just $35, emphasizing its practicality for widespread use.

Han *et al.*[76] introduced a supramolecular fluorescent architecture, based on the self-assembly of polyacrylic acid (PAA) and the small-molecule NBHN (*N*-butyl-4-hydrazino-1,8-naphthalimide). Through hydrogen bonding and π–π stacking interactions, PAA and NBHN generate hollow nanoparticles (PAA@NBHN), enhancing their water solubility, stability, sensitivity, and response time towards FA, compared to the free NBHN probe. The fluorescence mechanism is based on PET, where FA binding inhibits PET from the hydrazine group to the naphthalimide scaffold and triggers a fluorescence "turn-on" response; also, the hydrazine group has been used due to its capabilities of FA recognition, and the butyl group provides a hydrophobic nanocavity for FA binding. To further broaden its applicability, additional fluorescent molecules (MBNI and cresyl violet) were incorporated to produce colour-tuneable signals, enabling both aqueous and airborne FA detection. The platform was also adapted into practical formats, including paper-based sensors and colorimetric reagents, suitable for indoor air quality monitoring (Fig. 11). The use of readily available PAA makes the platform cost-effective and easy to produce.

Du *et al.*[77] developed a ratiometric fluorescent sensing nanoplatform (CDs/AuNCs@ZIF-8) integrating carbon dots (CDs) and gold nanoclusters (AuNCs) inside a zeolitic imidazolate framework (ZIF-8), in a hydroxylamine hydrochloride ($NH_2OH{\cdot}HCl$) medium, which represents an FA recognizer. This platform exhi-

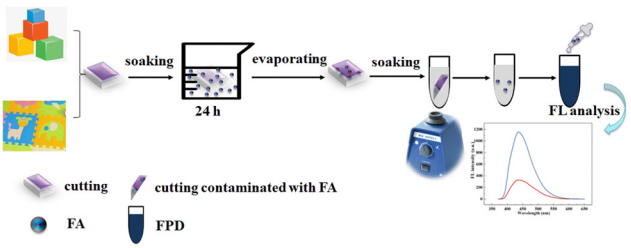

Fig. 10 Schematic procedure for FA sensing in toys. Reproduced from ref. 73 with permission from the Royal Society of Chemistry, copyright 2024.

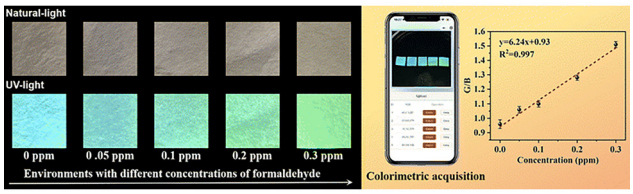

Fig. 11 Photographs of strip tests exposed to various FA concentrations in simulated air samples (left). RGB value acquisition with a smartphone and their linear correlation with FA concentration (right). Adapted from ref. 76 with permission from the Royal Society of Chemistry, copyright 2025.

Table 1 Summary of the optical sensors for formaldehyde detection and their optical properties

Sensing mechanism	Sensor	λ_{ex}, λ_{em}	Response time	LOD	Linear range	Selectivity	Solid-state use, reversibility	Real application	Source	Ref.
aza-Cope	TPE-FA	365 nm, 504 nm	60 min	0.036 ppb	0–1.6 ppb	Aldehydes, acids, ammonia	Yes, no	n.d.	Air	36
aza-Cope	Hydrazino-naphtha.-chitosan polymer	440 nm, 555 nm	<1 min	0.05 ppm	1–100 ppm	Acetaldehyde, cations, anions, salts, amino acids	No, no	Food and water samples	Aqueous solution	37
aza-Cope	PBD-FA	470 nm, 563 nm	180 min	1.31 ppb	0–3 ppm, 6–15 ppm	Aldehydes, anions, cations, salts, amino acids	No, no	Living HeLa cells	Aqueous solution	38
aza-Cope	HBT-FA	350 nm, 462/ 541 nm	3 h	12.31 ppm	0–900 ppm	*n*-Butyl aldehyde, GSH, amino acids, glucose, salts	Yes, no	Air, calf serum	Solution, air, serum	39
aza-Cope	TP-FA	305 nm, 442/ 488 nm	60 min	1.53 ppm	0–168 ppm	Aldehydes, methylglyoxal	Yes, no	n.d.	Solution, air	40
aza-Cope	ZIF-90-LW	380 nm, 438 nm	28 s	69.1 ppm	0–750 ppm	Aldehydes, acetone, ethyl acetate, H_2O_2, glucose	Yes, no	Strip test, gas phase	Solution, air	41
aza-Cope	Fluorescent aerogel	290 nm, 370 nm	n.d.	110 ppm	n.d.	VOCs, metal ions, anions	Yes, no	n.d.	Solution, air	42
aza-Cope	1-(10-Ethyl-10*H*-phenothiazin-3-yl) but-3-en-1-amine	365 nm, 400/ 505 nm	5 min	3 ppm	n.d.	Aldehydes, salts, O_2, H_2O_2, GSH, amino acids, VOCs, glucose	Yes, no	Food, soil, zebrafish, living cells	Solution, air	43
aza-Cope	PEI-FP	380/ 420 nm, 450/ 540 nm	<30 min	0.014 ppm	3–237 ppm	Benzaldehyde, solvents, CO, cations, anions	Yes, no	n.d.	Air	44
Formimine	NBD	485 nm, 545 nm	2 min	2.5 ppb	0–75 ppb	Aldehydes, acetone, amino acids	Yes, no	Plywood emission	Air	45
Formimine	CD@SiO_2-NH_2	360 nm, 466 nm	30 min	3 ppb	0–20 ppm	Aldehydes, VOCs	Yes, no	n.d.	Air	46
Formimine	d^{10}-MOFs CMERI-1 & CMERI-2	350 nm, 430 nm	1 min	18.6 ppb (CMERI-1), 41.7 ppb (CMERI-2)	2.3–8.4 ppb (1), 1.5–11.7 ppb (2), 0–70 ppm (gas)	Aldehydes	Yes, no	Food samples, water sources	Aqueous solution, vapor phase	47
Formimine	N-doped CDs	360 nm, 450 nm	n.d.	22 ppb	36–270 ppb	VOCs and common organic solvents	No, no	n.d.	Indoor air	48
Formimine	Phenylethynyl aniline	370 nm, 508 nm	20 min	0.023 ppm	0–30 ppm	Aldehydes, glycine, valine, VOCs, cations	No, no	River water	Polluted water	49
Formimine	Sodium ligninsulfonate derived CDs	420 nm, 532 nm	2–3 min	2.4 ppb	0–1.5 ppm	Cations, anions, methanol, formic acid	Yes, no	Indoor air	Solution, air	50
Formimine	Ethylenediamine – Eu^{3+} – UiO-66 MOF	280 nm, 615 nm	30 min	0.38 ppm	0–8 ppm	Poor, it responds to any aldehyde	Yes, no	Frozen shrimp tails	n.d.	51
Formimine	Naphthalimide derivative	415 nm, 550 nm	2 min	15 ppm	30–120 ppm	Aldehydes, anions, cations, amino acids	No, no	Food, living cells	Solution	52
Formimine	DCP5 copolymer	420 nm, 580 nm	1 min	0.04 ppb	n.d.	Aldehydes, ketones	Yes, yes	n.d.	Solution, air	53
Methylene hydrazine	HBQP capped CdTe/CdS QDs	385 nm, 540/ 666 nm	n.d.	0.015 ppm	0.03–0.84 ppm	Aldehydes, solvents, NH_3, acetic acid, L-cysteine, H_2O_2	Yes, no	n.d.	Aqueous solution, air	54

Table 1 *(Contd.)*

Sensing mechanism	Sensor	λ_{ex}, λ_{em}	Response time	LOD	Linear range	Selectivity	Solid-state use, reversibility	Real application	Source	Ref.
Methylene hydrazine	Pillar[5]arene derivative	365 nm, 450 nm	7.5 s	0.1 ppb	1.5–3.3 ppb	Aldehydes	Yes, no	n.d.	Air, DMF solution	55
Methylene hydrazine	Hydrazine modified NBD-Cl	470 nm, 550 nm	40 min	0.89 ppb	0.015–800 ppb	Acetaldehyde, salts, VOCs, ascorbic acid	No, no	Air samples	Air	56
Methylene hydrazine	DHT	385 nm, 508 nm	13 min	8.7 ppb	0–600 ppb	Aldehydes, hydroquinone, glucose, H_2O_2	Yes, no	Gas, cell imaging	Air, solution	57
Methylene hydrazine	Naphthalimide derivative	350 nm, 550 nm	1 min	0.3 ppb	6–27 ppb	Aldehydes, organic solvents	Yes, es	Air, aquatic products, HeLa cells	Seafood, air, living cells	58
Methylene hydrazine	Nap-NH_2	435 nm, 551 nm	30 min	1.9 ppb	0–2.4 ppm	Aldehydes, TFA	Yes, no	Simulated industrial scenario	Air	59
Methylene hydrazine	Quinolimide	445 nm, 540 nm	50 min	0.051 ppm	0–5.4 ppm	Ions, amino acids, acetaldehyde, glyoxal, acetone, H_2O_2	Yes, no	Strip test, living cells	Solution	60
Methylene hydrazine	OPTY	422 nm, 465 nm	22 min	0.8 ppb	0–300 ppb	Aldehydes, anions, cations, amino acids	Yes, no	Food	Solution	61
Methylene hydrazine	BCP2-N	440 nm, 535 nm	10 min	51 ppb	n.d.	Aldehydes, ketones	No, no	n.d.	Solution	62
Methylene hydrazine	W-1a	395 nm, 528 nm	13 min	0.027 ppm	0–4.5 ppm	Aldehydes, anions, cations, thiols, ROS	Yes, no	Indoor air, seafood products	Solution, air	63
Other	Dopamine, glycine and sucrose	420 nm, 485 nm	30 min	7.2 ppm (sol.), 0.4 ppm (gas)	15–150 ppm	Aldehydes, acetone, methanol, toluene	Yes, no	Air	Aqueous solution, air	64
Other	SAM	370 nm, 435/ 440 nm	30 min	<1 ppm	n.d.	Aldehydes, VOCs, organic solvents	Yes, yes	n.d.	Aqueous solution	65
Other	HNU-44	394 nm, 436 nm	20 s	27.41 ppb (sol.), 2.61 ppb (gas)	n.d.	Aldehydes, toluene, ammonia	No, no	Air, fish	Aqueous solution, air	66
Other	*N*-Hydroxy methylation	340 nm, 420 nm	<1 min	22.5 ppb	18–245 ppb	Aldehydes	No, yes	n.d.	n.d.	67
Other	PHTA	395 nm, 510/ 640 nm	10 min	0.47 ppb	14.4–27.6 ppm	Acetaldehyde, toluene, xylene	Yes, no	n.d.	DMSO solution	68
Other	Leuco-Fuchsin on PMMA-Naflon	n.d., 575 nm	15 min	0.02–0.03 ppm	0.03–5.5 ppm	Aldehydes, methanol, acetone	Yes, no	Industrial paper	Air	69
Other	Lignin derived multicolor carbon dots	380 nm, 493 nm	1 min	7.4 ppb	0.02–1 ppm	Cations	No, no	n.d.	n.d.	70
Other	GSH-CdTe	310 nm, 522 nm	2 min	0.28 ppb	0–2.4 ppm	Aldehydes, cations, anions	No, no	n.d.	Solution	71
Other	Perylene diimide	405 nm, 500/ 650 nm	10 min	3.7 ppb	0–900 ppb	Alcohols, hydrocarbons, ammonia	Yes, yes	n.d.	Air	72
Other	FPD	365 nm, 435 nm	14 min	2.03 ppb	n.d.	Aldehydes, cations, salts	No, yes	Toys, water sample	Solution	73

Table 1 *(Contd.)*

Sensing mechanism	Sensor	λ_{ex}, λ_{em}	Response time	LOD	Linear range	Selectivity	Solid-state use, reversibility	Real application	Source	Ref.
Other	Eu-MOF	360 nm, 460/ 615 nm	2 s	5.83 ppb	3–30 ppb	Poor, it is sensitive to other substances (Hg^{2+}, Cd^{2+})	Yes, no	filter paper	Solution	74
Other	DDL	410 nm, 515 nm	20 min	0.03 ppm	0.1–3 ppm	Fat ad proteins	No, no	Milk samples	Milk	75
Other	PAA@NBHN	395 nm, 545 nm	10 min	0.027 ppm	0–0.3 ppm	Aldehydes, ions	Yes, no	Indoor air, life products	Solution, air	76
Other	CDs/AuNCs@ ZIF-8 + $NH_2OH{\cdot}HCl$ nanoplatform	390 nm, 468/ 615 nm	1 min	0.013 ppm	0.48–0.63 ppm, 0.63–1.20 ppm	VOCs, anions, cations	Yes, no	Indoor air, building materials, food	Solution, air	77

n.d.: not determined.

bits initial pink fluorescence due to the AIE of AuNCs and IFE between AuNCs and CDs. The reaction between FA and $NH_2OH{\cdot}HCl$ leads to a Schiff base and releases HCl, which triggers the degradation of ZIF-8, thus liberating CDs and AuNCs. This results in a shift to blue fluorescence, due to the CD dispersion, enabling ratiometric detection of FA.

The platform shows excellent sensitivity, with a detection limit of 13 ppb and a rapid response time <1 min in real samples. To facilitate real-world applications, test strips and wearable hydrogel films were implemented applying detection by smartphone for visual, practical and on-site FA detection.

Table 1 summarizes the main features of the FA probes analysed in this review. Among the various sensing strategies, methylene-hydrazine-based systems currently offer the most favorable balance between sensitivity and selectivity, particularly when integrated with structured platforms such as QDs, MOFs, and pillararenes. Several of these sensors achieve sub-ppb detection limits (*e.g.*, 0.015 ppm with CdTe/CdS QDs, 0.1 ppb with pillar[5]arene derivatives, and 0.3 ppb with naphthalimide derivatives) while maintaining good selectivity, especially in the presence of aldehydes and VOCs. Notably, the pillar[5]arene-based sensor combines an ultra-low LOD with a fast response time (<10 s), making it suitable for real-time applications. In contrast, aza-Cope-based probes—despite their excellent specificity for formaldehyde *via* covalent binding mechanisms (*e.g.*, PEI-FP, LOD 0.014 ppm)—often lack reversibility and suffer from limited selectivity in complex environments. Formimine-based systems also show potential, particularly those coupled with carbon dots or MOFs, although they typically exhibit slightly higher LODs and broader cross-reactivity.

Top-performing systems, in terms of sensitivity, time response, and real-world applicability, include: (i) pillar[5]arene derivative (0.1 ppb, 7.5 s); (ii) DCP5 copolymer (0.04 ppb, 1 min), notable for its reversibility; and (iii) naphthalimide derivative (0.3 ppb, 1 min), validated in air, food, and biological matrices. Additional promising platforms include the CDs/AuNCs@ZIF-8 + $NH_2OH{\cdot}HCl$ nanoplatform, which performs well across air, food, and building materials, and the sodium ligninsulfonate-derived carbon dots (LOD: 2.4 ppb), designed for indoor air monitoring.

Most of the sensors analyzed exhibit emission maxima in the visible range (typically 500–600 nm), enabling direct optical readouts, including smartphone-assisted or naked-eye detection. Moreover, many systems tested in aqueous environments—particularly those based on chitosan, MOFs, or carbon dots—demonstrate good water compatibility, supporting their use in food safety, environmental monitoring, and bioanalysis. Conversely, some aza-Cope and solid-state platforms display limited aqueous solubility, which may require further chemical modification for liquid-phase applications.

Despite these advancements, several technical limitations persist:

• Irreversibility: covalent mechanisms such as aza-Cope, hydrazone, or imine formation often prevent sensor regeneration, limiting reuse.

• pH dependence: many sensors perform poorly under variable pH, particularly in biological or environmental matrices. Future work should prioritize pH-insensitive probes or buffered systems.

• Reduced solid-state sensitivity: sensors that perform well in solution often exhibit reduced efficiency when immobilized on paper strips or membranes, due to limited diffusion or quenching effects.

• Cross-selectivity and matrix effects: in real-world environments, coexisting VOCs or reactive species can interfere, emphasizing the need for multichannel systems or data-driven approaches for analyte discrimination.

• Lack of integration and scalability: only a few systems are compatible with portable or smartphone-based formats, and the absence of standardization in calibration and packaging hinders commercial translation.

Addressing these bottlenecks will be critical for advancing formaldehyde sensing technologies toward broader and more reliable real-world use.

Conclusions and future perspectives

Although formaldehyde has been recognized as extremely toxic and its use has therefore been restricted and regulated by different laws, it is still likely to be found in both external and internal environments. The high reactivity and the formation in various industrial processes make FA a molecule that, probably, will not disappear in the next future. For this reason, the possibility to monitor the FA concentration in real time by fast and easy analysis is of extreme actuality and importance. Detection by optical probes matches these criteria. In the present review, we highlighted different sensing mechanisms in which FA reacts covalently with a molecule (optical or fluorescent probe), leading to the formation of a new compound, which has different UV-Vis or emission spectrum with respect to the starting probe. This change in optical features can also be quantified, leading to the possibility to monitor FA concentration.

In this context, sensing by optical probes shows some important aspects that an ideal sensor should satisfy.

Selectivity

The possibility of having a false-positive response due to the interaction of the probe with other analytes must be reduced to zero (if possible). Most of the probes, in fact, contain a nucleophilic group that reacts with FA. However, this reaction is not always selective for FA, and it can also occur with other analytes containing carbonyl groups. In this context, a supramolecular approach can probably increase the performance, by enabling the design of probes (receptors) with different recognition points for FA, thereby avoiding the possibility to interact with other analytes.[24,30,78]

Sensitivity (limit of detection)

Due to the low concentration of FA allowed for indoor and outdoor environments (few ppm and ppb levels, respectively), a good probe/sensor requires the ability to detect FA at trace levels (ppt-ppb). This feature is extremely important, and the optical characteristics of the fluorophore, mainly in terms of emission quantum yield, are crucial. Organic fluorophores having these characteristics are, in general, BODIPYs, rhodamines, naphthalimides, and porphyrins. Therefore, these building blocks can be employed to reach low limits of detection.

Range of linearity

Sensors having the possibility to detect FA in a concentration range into one order of magnitude are not practical. The FA concentration can undergo variation larger than two or three orders of magnitude. Thus, an ideal sensor must detect FA in the ppt-ppm range, very larger with respect to most of the optical probes analyzed in this review.

Timing of the response

In general, an ideal sensor must indicate the presence of the target analyte immediately. In particular, if the analyte is a toxic molecule, this aspect is essential. For this reason, the possibility to detect FA immediately, or in few seconds, is a crucial feature. The reaction between FA and the nucleophilic group contained in the probe can be slow (different minutes) and can be a function of temperature and concentration. The supramolecular approach, as previously described, can solve this problem, leading to an immediate response of the probe to the analyte.

Author contributions

Investigation: A. Cavallaro, R. Santonocito, A. Pappalardo, N. Tuccitto, and G. Trusso Sfrazzetto; supervision: A. Cavallaro and G. Trusso Sfrazzetto; writing – original draft: A. Cavallaro and G. Trusso Sfrazzetto; writing – review and editing: G. Trusso Sfrazzetto.

Conflicts of interest

There are no conflicts to declare.

Data availability

No primary research results, software or code have been included and no new data were generated or analysed as part of this review.

Acknowledgements

This work has been partially funded by the European Union (NextGeneration EU) through the MUR-PNRR project SAMOTHRACE (ECS00000022).

References

1 G. Reuss, W. Disteldorf, A. O. Gamer and A. Hilt, *Ullmann's Encyclopedia of Industrial Chemistry*, WILEY-VCH, Weinheim, 2000.
2 K. J. Bruemmer, T. F. Brewer and C. J. Chang, *Curr. Opin. Chem. Biol.*, 2017, **39**, 17–23.
3 K. Lu, S. Craft, J. Nakamura, B. C. Moeller and J. A. Swenberg, *Chem. Res. Toxicol.*, 2012, **25**, 664–675.
4 Z. Tong, C. Han, W. Luo, H. Li, H. Luo, M. Qiang, T. Su, B. Wu, Y. Liu, X. Yang, Y. Wan, D. Cui and R. He, *Ageing Res. Rev.*, 2013, **35**, 583–596.
5 X. Tang, Y. Bai, A. Duong, M. T. Smith, L. Li and L. Zhang, *Environ. Int.*, 2009, **35**, 1210–1224.
6 Y. Li, N. Chen, D. Deng, X. Xing, X. Xiao and Y. Wang, *Sens. Actuators, B*, 2017, **238**, 264–273.
7 S. Kim, *Bioresour. Technol.*, 2009, **100**, 744–748.
8 T. W. Zinn, D. Cline and W. F. Lehmann, *For. Prod. J.*, 1990, **40**, 15–18.
9 R. Koppmann and J. Wildt, in *Volatile Organic Compounds in the Atmosphere: an overview*, ed. R. Koppmann, Blackwell Publishing Ltd., Oxford, 2007, pp. 1–32.
10 M. Tasooji and C. E. Fraizer, *ACS Sustainable Chem. Eng.*, 2021, **9**, 207–215.
11 D. Trapp, K. M. Cooke, H. Fischer, B. Bonsang, R. U. Zitzelsberger, R. Seuwen, C. Schiller, T. Zenker, U. Parchatka, T. V. Nunes, C. A. Pio, A. C. Lewis, P. W. Seakins and M. J. Pilling, *Chemosphere*, 2001, **3**, 295–307.
12 K. Griesbaum, V. Miclaus and I. C. Jung, *Environ. Sci. Technol.*, 1998, **32**, 647–649.
13 E. Hedberg, A. Kristensson, M. Ohlsson, C. Johansson, P.-Å. Johansson, E. Swietlicki, V. Vesely, U. Wideqvist and R. Westerholm, *Atmos. Environ.*, 2002, **36**, 4823–4837.
14 M. Hauptmann, K. Straif and B. Pesch, in *Handbuch der Umweltmedizin*, ed. H.-E. Wichmann, H.-W. Schlipköter and G. Füllgraff, ECOMED-Verlag, Landsberg, 2006, pp 1–28.
15 O. Merk and G. Speit, *Environ. Mol. Mutagen.*, 1998, **32**, 260–268.
16 X. Q. Zhao and Z. Q. Zhang, *Talanta*, 2009, **80**, 242–245.
17 F. X. Li, J. Lu, Y. J. Xu, Z. Q. Tong, C. L. Nie and R. Q. He, *Prog. Biochem. Biophys.*, 2008, **35**, 393–400.
18 H. Reingruber and L. B. Pontel, *Curr. Opin. Toxicol.*, 2018, **9**, 28–34.
19 Z. Yuan, C. Yang and F. Meng, *Chemosensors*, 2021, **9**, 179.
20 ATSDR's substance priority list. Agency for Toxic Substances and Disease Registry. **https://www.atsdr.cdc.gov/programs/substance-priority-list.html#cdc_program_profile_strategies-substance-priority-list**, (accessed November 24, 2020).
21 D. Kukkar, K. Vellingiri, R. Kaur, S. Bhardwaj, A. Deep and K. Kim, *Nano Res.*, 2019, **12**, 225–246.
22 C. Liao, J. Shi, M. Zhang, R. Dalapati, Q. Tian, S. Chen, C. Wang and L. Zang, *Mater. Adv.*, 2021, **2**, 6213–6245.
23 Y. Yang, Y. Hao, L. Huang, Y. Luo, S. Chen, M. Xu and W. Chen, *Molecules*, 2024, **29**, 327.
24 E. S. Cross, L. R. Williams, D. K. Lewis, G. R. Magoon, T. B. Onasch, M. L. Kaminsky, D. R. Worsnop and J. T. Jayne, *Atmos. Meas. Tech.*, 2017, **10**, 3575–3588.
25 A. Bi, S. Yang, M. Liu, X. Wang, W. Liao and W. Zeng, *RSC Adv.*, 2017, **7**, 36421–36432.
26 S. K. Manna, T. K. Achar and S. Mondal, *Anal. Methods*, 2021, **13**, 1084–1100.
27 S. Pan, S. Roy, N. Choudhury, P. P. Behera, K. Sivaprakasam, L. Ramakrishnan and P. De, *Sci. Technol. Adv. Mater.*, 2022, **23**, 49–63.
28 S. Roy, S. Pan and P. De, *Sci. Technol. Adv. Mater.*, 2024, **25**, 2423597.
29 E. Butera, A. Zammataro, A. Pappalardo and G. Trusso Sfrazzetto, *ChemPlusChem*, 2021, **86**, 681–695.
30 D. Zhang, D. Liu, M. Li, Y. Yang, Y. Wang, H. Yin, J. Liu, B. Jia and X. Wu, *Anal. Chim. Acta*, 2018, **1033**, 180–184.
31 G. Trusso Sfrazzetto, C. Satriano, G. A. Tomaselli and E. Rizzarelli, *Coord. Chem. Rev.*, 2016, **311**, 125–167.
32 N. Tuccitto, L. Fichera, R. Ruffino, V. Cantaro, G. Sfuncia, G. Nicotra, G. Trusso Sfrazzetto, G. Li-Destri, A. Valenti, A. Licciardello and A. Torrisi, *ACS Appl. Nano Mater.*, 2021, **4**, 6250–6256.
33 N. Tuccitto, G. Catania, A. Pappalardo and G. Trusso Sfrazzetto, *Chem. – Eur. J.*, 2021, **27**, 13715–13718.
34 R. Puglisi, A. Pappalardo, A. Gulino and G. Trusso Sfrazzetto, *ACS Omega*, 2019, **4**, 7550–7555.
35 L. Legnani, R. Puglisi, A. Pappalardo, M. A. Chiacchio and G. Trusso Sfrazzetto, *Chem. Commun.*, 2020, **56**, 539–542.
36 X. Zhao, C. Ji, L. Ma, Z. Wu, W. Cheng and M. Yin, *ACS Sens.*, 2018, **3**, 2112–2117.
37 P. Li, D. Zhang, Y. Zhang, W. Lu, W. Wang and T. Chen, *ACS Sens.*, 2018, **3**, 2394–2401.
38 X. Yang, L. He, K. Xu, Y. Yang and W. Lin, *New J. Chem.*, 2018, **42**, 12361–12364.
39 Y. Zhou, J. Yan, N. Zhang, D. Li, S. Xiao and K. Zheng, *Sens. Actuators, B*, 2018, **258**, 156–162.
40 B. Zhai, Y. Zhang, Z. Hu, J. He and J. Liu, *Dyes Pigm.*, 2019, **171**, 107743.
41 L. Mengwen, S. Ao, L. Yueqi, Z. Hao, H. Xiaohui, L. Xueliang, S. Xinchao and Y. Yunxu, *Anal. Methods*, 2020, **12**, 3748–3755.
42 Q. Zheng, H. Zhang, J. Liu, L. Xiao, Y. Ao and M. Li, *Microporous Mesoporous Mater.*, 2021, **325**, 111208.
43 J. Ai, Y. Cui, M. Ren, K. Liu, S. Wang, Q. Wu, X. Wang and F. Kong, *Microchem. J.*, 2024, **203**, 110902.
44 Y. Chen, P. Zong, X. Wang, J. Luo, R. Zhang and K. Liu, *J. Mol. Struct.*, 2025, **1319**, 139543.
45 A. Gangopadhyay, K. Maiti, S. S. Ali, A. K. Pramanik, U. N. Guria, S. K. Samanta, R. Sarkar, P. Datta and A. K. Mahapatra, *Anal. Methods*, 2018, **10**, 2888–2894.

46 W. Yang, G. Zhang, J. Ni and Z. Lin, *Microchim. Acta*, 2020, **187**, 137.
47 S. Bej, S. Mandal, A. Mondal, T. K. Pal and P. Banerjee, *ACS Appl. Mater. Interfaces*, 2021, **13**, 25153–25163.
48 Y. Tachapermpon, P. Muangphrom, P. Pataranutaporn, W. Chaiworn and W. Surareungchai, *Plant Nano Biol.*, 2022, **2**, 100015.
49 X. Z. Tan, M. Y. Hua, S. Y. Wang, L. Xu, G. F. Zhang and X. L. Gou, *ChemistrySelect*, 2024, **9**, e202400140.
50 F. Ma, T. Zhang, H. Xing, L. Wang, H. Hu, Y. Zhang and D. Chen, *Mater. Lett.*, 2024, **362**, 136223.
51 W. Bai, C. Li, Z. Zhao, H. Chai and L. Gao, *Spectrochim. Acta, Part A*, 2024, **310**, 123937.
52 Q. Wang, M. Xie, W. Chen, M. Shen, Q. Zhang, H. Guo, Y. Tang, W. Luo and G. Zhou, *J. Mol. Struct.*, 2025, **1321**, 140184.
53 S. Roy, S. Pan, S. Sivaram and P. De, *Sci. Technol. Adv. Mater.*, 2025, **26**(1), 2469493.
54 I. Ahmada, Z. Zhoua, H.-Y. Lia and S.-Q. Zang, *Sens. Actuators, B*, 2020, **304**, 127379.
55 Q. Lin, Y.-Q. Fan, G.-F. Gong, P.-P. Mao, J. Wang, X.-W. Guan, J. Liu, Y.-M. Zhang, H. Yao and T.-B. Wei, *ACS Sustainable Chem. Eng.*, 2018, **6**, 8775–8781.
56 G. Hongwei, L. Guoqiang, Y. Ranhao, S. Zhenli, C. Hongxia, Y. Long, S. Pengchen, S. Mingtai, K. A. Alamry, H. M. Marwani and W. Suhua, *Microchem. J.*, 2020, **156**, 104793.
57 Y. Cao, Z. Teng, J. Zhang, T. Cao, J. Qian, J. Wang, W. Qin and H. Guo, *Sens. Actuators, B*, 2020, **320**, 128354.
58 X. Lu, R. Li, B. Han, H. Ma, X. Hou, Y. Kang, Y. Zhang and J.-J. Wang, *ACS Appl. Mater. Interfaces*, 2021, **13**, 13792–13801.
59 H. Ye, Y. Ke, C. Yue, P. Xie, R. Sheng and L. Zeng, *Dyes Pigm.*, 2022, **207**, 110782.
60 H. Cao, J. Yang, Y. Zhang, W. Qu and L. Jia, *J. Photochem. Photobiol., A*, 2023, **444**, 115023.
61 H. Ye, Y. Yang, L. Jiang, T. Zhe, J. Xu and L. Zeng, *Chin. Chem. Lett.*, 2025, DOI: **10.1016/j.cclet.2025.110840**.
62 S. Pan, S. Roy and P. De, *Macromol. Chem. Phys.*, 2025, **226**, 2400434.
63 X. Wang, Z. Huang, C. Sui, M. Xu, J. Ru and X. Sun, *Microchem. J.*, 2025, **209**, 112672.
64 C. Martínez-Aquino, A. M. Costero, S. Gil and P. Gaviña, *Molecules*, 2018, **23**, 2646.
65 M. Li, K. Xie, G. Wang, J. Zheng, Y. Cao, F. Wei, H. Tu and J. Tang, *Langmuir*, 2021, **37**, 5916–5922.
66 Y. Fang, G. Ren, M. Li, Y. Yang, D.-Y. Guo and Q. Pan, *Sens. Actuators, B*, 2021, **349**, 130726.
67 M.-Y. Yu, L.-H. Xu, Z. Zhang, Z. Qiao, P. Su, P. Wang and T.-Z. Xie, *Inorg. Chem.*, 2022, **61**, 20200–20205.
68 T.-B. Wei, L.-R. Dang, J.-P. Hu, Y. Jia, Q. Lin, H. Yao, B. Shi, Y.-M. Zhang and W.-J. Qu, *New J. Chem.*, 2022, **46**, 20658–20663.
69 M. del Mar Darder, M. Bedoya, L. A. Serrano, M. A. Alba and G. Orellana, *Sens. Actuators, B*, 2022, **353**, 131099.
70 Y. Li, M. Hu, K. Liu, S. Gao, H. Lian and C. Xu, *Ind. Crops Prod.*, 2023, **192**, 116006.
71 J. Hou, X. Liu, D. Zhao, Z. Li, Y. Ma, H. Luo, J. Lei, C. Hou and D. Huo, *Microchem. J.*, 2023, **190**, 108647.
72 C. Liao, M. Zhang, Q. Tian, X. Yang, J. Shi, S. Chen, Y. Che, C. Wang and L. Zang, *Sens. Actuators, B*, 2023, **375**, 132861.
73 W. Fan, S. Yang, Y. Kou, X. Wang, Q. Zhang and H. Tan, *Anal. Methods*, 2024, **16**, 458–464.
74 J. Zhu, L. Fan, W. Li, X. Qi, C. Sun, W. Li and Z. Chang, *J. Photochem. Photobiol., A*, 2024, **452**, 115583.
75 A. N. S. Cadeado, C. C. S. Machado and S. G. Silva, *Food Chem.*, 2025, **464**, 141583.
76 Q. Han, R. Sun, X. Wang, L. Ning, L. Chen, X. Ling and X. Guan, *J. Mater. Chem. C*, 2025, **13**, 2459.
77 M. Du, M. Song, S. Hou, Y. Zhang, H. Lv, S. Zhao, H. Du and H. Guo, *Microchim. Acta*, 2025, **192**, 96.
78 R. Puglisi, P. G. Mineo, A. Pappalardo, A. Gulino and G. Trusso Sfrazzetto, *Molecules*, 2019, **24**, 2160.